Binary Interaction Energy Densities for Blends of Styrene/Acrylonitrile Copolymers with Methyl Methacrylate/*n*-Alkyl Acrylate Copolymers

Shixiong Zhu and Donald R. Paul*

Department of Chemical Engineering and Texas Materials Institute, The University of Texas at Austin, Austin, Texas 78712

Received May 20, 2002; Revised Manuscript Received July 26, 2002

ABSTRACT: Isothermal miscibility maps for blends of styrene−acrylonitrile (SAN) copolymers with methyl methacrylate (MMA) copolymers containing *n*-alkyl acrylates (xA) have been determined at 120 °C. The miscibility region increases and then decreases as the size of the *n*-alkyl pendant group increases. Binary interaction energy densities for various monomer unit pairs were evaluated from the miscibility data by both the copolymer/critical molecular weight and the copolymer composition mapping approaches using the Flory−Huggins theory combined with the binary interaction model. Values of binary interaction energy densities obtained from both approaches, with the aid of an appropriate data fitting algorithm, agreed very well with each other. Trends in binary interaction energy densities involving the various *n*-alkyl acrylate units, $B_{MMA/xA}$, $B_{S/xA}$, and $B_{AN/xA}$, could be roughly predicted by the simple solubility parameter theory. Trends in the deviations from the geometric mean assumption, k_{ij}, were qualitatively explained in terms of monomer molecular characteristics, especially polarity, monomer size, and first ionization potential.

Introduction

Poly(methyl methacrylate) (PMMA) is miscible with styrene−acrylonitrile copolymers (SAN) when the acrylonitrile (AN) content is between 10 and 32 wt %.[1−12] For commercial applications, methyl methacrylate (MMA) is often copolymerized with other monomers such as acrylates, acrylonitrile, styrene, and butadiene for various reasons. For example, acrylate monomers are commonly incorporated into commercial PMMA materials to stabilize against depolymerization since acrylate polymers have much higher ceiling temperatures than methacrylate homopolymers and are very stable under normal processing conditions. The addition of other comonomers in MMA-based polymers alters the miscibility window with SAN copolymers, and several such systems have been reported previously in the literature. For example, Merfeld et al. examined blends of SAN with copolymers of methyl methacrylate with phenyl maleimide, tribromophenyl maleimide, and pentabromobenzyl acrylate.[13,14] Gan investigated blends of SAN copolymers with copolymers of methyl methacrylate with glycidyl methacrylate and *tert*-butyl methacrylate.[15] Nishimoto et al. studied blends of SAN copolymers with methyl methacrylate copolymers containing cyclohexyl methacrylate, phenyl methacrylate, and *tert*-butyl methacrylate.[2] Chu et al. studied blends of SAN with methyl methacrylate copolymers containing tribromostyrene, 2-hydroxyethyl methacrylate, 4-methacryloxyethyl trimellitic anhydride, ethyl acrylate (EA), and *n*-butyl acrylate (nBA).[10−12] Chu and Paul observed that the miscibility region with SAN for MMA−nBA copolymers is larger than that for MMA−EA copolymers.[10] This result is very interesting since it is contradictory to what one may think intuitively. The first objective of this study is to explore systematically how the *n*-alkyl chain length affects the amount of *n*-alkyl acrylate (xA) that can be incorporated into copolymers with MMA while maintaining miscibility with SAN copolymers.

* To whom correspondence should be addressed. E-mail: drp@che.utexas.edu.

The binary interaction energy densities between the six repeat unit pairs represented in these copolymer−copolymer blends, i.e., S/MMA, S/AN, MMA/AN, MMA/xA, S/xA, and AN/xA, can be determined by observing the phase boundaries (molecular weight, copolymer composition, temperature) that separate the miscible from immiscible regions for mixtures of SAN with MMA-*co*-*n*-alkyl acrylate copolymers and by interpreting the results within the framework of an appropriate thermodynamic theory.[10] This copolymer composition mapping method has been successfully used in a number of prior studies to determine binary interaction energy densities.[10−12,14,16−19] However, this approach has some drawbacks which prompted interest by this laboratory in the so-called copolymer/critical molecular weight method as a potentially more accurate alternative.[11,12,20] A further objective of this study is to evaluate and compare interaction energy densities between repeat unit pairs by both approaches where possible. The relationship between the interaction energies for the MMA/xA, S/xA, and AN/xA pairs and *n*-alkyl chain length and the trends in interaction energy densities will also be discussed.

Background and Theory

Three strategies will be used in this study to obtain the binary interaction energy density information; each requires the use of an appropriate thermodynamic theory of mixing to model and predict polymer blend phase behavior. The Gibbs free energy of mixing per unit volume (Δg_{mix}) can be simply modeled by the Flory−Huggins (FH) theory for a blend of monodisperse homopolymers A and B,[21,22] i.e.where B is the binary

$$\Delta g_{mix} = B\phi_A\phi_B + RT\left[\frac{\rho_A\phi_A \ln \phi_A}{M_A} + \frac{\rho_B\phi_B \ln \phi_B}{M_B}\right] \quad (1)$$

interaction energy density, R is the universal gas constant, T is the absolute temperature, and ϕ_i, ρ_i, and M_i are the volume fraction, density, and molecular weight of component i, respectively. The first term in

10.1021/ma020770q CCC: $22.00
Published on Web 09/13/2002

eq 1 is a van Laar type energetic interaction, while the second term is the combinatorial entropy of mixing. Therefore, B includes the contributions of the heat of mixing plus any other noncombinatorial effects. As pointed out by Sanchez et al. recently,[23] the FH model is more useful than is generally recognized even though far more sophisticated theories are rapidly evolving. The critical interaction energy at the boundary between miscibility and immiscibility, where the energy and entropy terms in eq 1 are balanced, is given by the following expression that treats polydispersity properly for most polydisperse polymers:[24−29]

$$B_{\text{critical}} = \frac{RT}{2}\left(\sqrt{\frac{\rho_A}{(\bar{M}_W)_A}} + \sqrt{\frac{\rho_B}{(\bar{M}_W)_B}}\right)^2 \tag{2}$$

where $(\bar{M}_w)_i$ is the weight-average molecular weight of polymer i. This equation is widely used in the so-called critical molecular weight method to determine the interaction energy density information.[10−12,24,30−33]

A second approach to evaluating the interaction energy is the well-known copolymer composition mapping in which the region of copolymer compositions where miscible blends are formed is determined experimentally[10−14,17−19,34] and then analyzed with the aid of the binary interaction model.[30,35,36] The binary interaction model considers multiple pairwise repeating unit interactions that may occur both intermolecularly and intramolecularly; this model has proven to be quite successful, at least when strong specific interactions are absent.[37] In this model, the net interaction energy density B in eq 1 is expressed in terms of the interactions between the various pairs of monomer units, B_{ij}, involved and their volume fractions, ϕ_i, in the copolymer. For a blend of a copolymer, consisting of monomers MMA and xA, with SAN copolymers of interest here, this model can be written as

$$B = B_{\text{S/MMA}}\phi'_{\text{S}}\phi''_{\text{MMA}} + B_{\text{S/xA}}\phi'_{\text{S}}\phi''_{\text{xA}} + B_{\text{AN/MMA}}\phi'_{\text{AN}}\phi''_{\text{MMA}} + B_{\text{AN/xA}}\phi'_{\text{AN}}\phi''_{\text{xA}} - B_{\text{S/AN}}\phi'_{\text{S}}\phi'_{\text{AN}} - B_{\text{MMA/xA}}\phi''_{\text{MMA}}\phi''_{\text{xA}} \tag{3}$$

where ϕ'_{S}, ϕ'_{AN} are the volume fractions of monomers S, AN in the SAN copolymer, ϕ''_{MMA}, ϕ''_{xA} are the volume fractions of monomers MMA, xA in the copolymer of MMA with xA, and B_{ij} is the interaction between monomer units i and j, respectively. The copolymer composition mapping method uses eq 3 combined with an appropriate, thermodynamic theory such as eq 1. It is quite useful since it can be used to determine several interaction energy densities at the same time with relatively good accuracy. However, as we have noted previously,[20] one of the disadvantages of this approach is that when several binary interaction energies are determined from the same data set, accuary can be compromised by compensation effects. This can be clearly seen in later discussions.

A third approach to determining the interaction energy density, called the copolymer/critical molecular weight method,[11,12,20] combines the first two strategies. In this paper, blends of monodisperse homopolymers of PMMA with MMA/xA copolymers and blends of monodisperse homopolymers of PS with S/xA copolymer are studied by this quite powerful approach. For these two blend systems, eq 3 can be simplified to the following

$$B = B_{\text{S/xA}}\phi'^{\,2}_{\text{xA}} \tag{4}$$

$$B = B_{\text{MMA/xA}}\phi''^{\,2}_{\text{xA}} \tag{5}$$

where B represents the net interaction energy density for each blend system, ϕ'_{xA} is the volume fraction of xA in the S/xA copolymer, and ϕ''_{xA} is the volume fraction of xA in the MMA/xA copolymer, respectively. The equations that describe the boundary between miscibility and immiscibility at a given temperature are obtained by combining eqs 2 and 4 (or 5), i.e.,

$$\phi'_{\text{xA}} = \sqrt{\frac{B_{\text{critical}}}{B_{\text{S/xA}}}} \tag{6}$$

$$\phi''_{\text{xA}} = \sqrt{\frac{B_{\text{critical}}}{B_{\text{MMA/xA}}}} \tag{7}$$

Thus, a plot of ϕ'_{xA} (or ϕ''_{xA}) vs $\sqrt{B_{\text{critical}}}$ leads to a diagram where miscible blends are separated from the immiscible blends by a straight line passing through the origin with a slope of $1/\sqrt{B_{\text{MMA/xA}}}$ or $1/\sqrt{B_{\text{S/xA}}}$. As we mentioned earlier, this approach is simpler and more accurate because only one interaction energy is obtained from a given data set. We have made extensive use of this approach recently.[11,12,20] However, it should be noted that only positive binary interaction energies can be determined by this method, and at very low molecular weights of the monodisperse homopolymer end groups can become an issue.[24]

The interaction parameters, B, in the Flory−Huggins framework can be translated into the bare interaction energy, ΔP^*, of the Sanchez−Lacombe lattice fluid framework and vice versa by the following[9,38,39]

$$B = \tilde{\rho}\Delta P^* + \left\{[P_2^* - P_1^* + (\phi_2 - \phi_1)\Delta P^*] + \frac{RT}{\tilde{\rho}}\left(\frac{1}{r_1^0 v_1^*} - \frac{1}{r_2^0 v_2^*}\right) - RT\left(\frac{\ln(1-\tilde{\rho})}{\tilde{\rho}^2} + \frac{1}{\tilde{\rho}}\right)\left(\frac{1}{v_1^*} - \frac{1}{v_2^*}\right)\right\}^2 \Big/ \left\{\frac{2RT}{v^*}\left[\frac{2\ln(1-\tilde{\rho})}{\tilde{\rho}^3} + \frac{1}{\tilde{\rho}^2(1-\tilde{\rho})} + \frac{(1-1/r)}{\tilde{\rho}^2}\right]\right\} \tag{8}$$

With recognized limitations, solubility parameters can be useful for estimating binary interaction energies in some cases. Scatchard and Hildebrand introduced the notion that the energy of a binary liquid mixture can be expressed as a quadratic function of the volume fractions of the component interactions.[40,41] In general, for random mixing, B_{ij} can be written as[40−42]

$$B_{ij} = C_{ii} - 2C_{ij} + C_{jj} \tag{9}$$

where C_{ii} and C_{jj} are the cohesive energy densities of the pure-component homopolymers and C_{ij} refers to interactions between unlike pairs. The geometric mean assumption based on the work of Berthelot and London is often invoked to account for the cross-interaction term, C_{ij}, for the unlike interaction.[43,44] This assumption states that

$$C_{ij} = \delta_i\delta_j \tag{10}$$

where $\delta_i = \sqrt{C_{ii}}$ and $\delta_j = \sqrt{C_{jj}}$ represent the solubility

parameters of pure component i and pure component j, respectively. Combining eqs 9 and 10 leads to the following relation for estimating B_{ij} from pure component properties

$$B_{ij} = (\delta_i - \delta_j)^2 \tag{11}$$

However, this is only a rough approximation since the geometric mean assumption is strictly applicable only for nonpolar systems where the interaction forces are dispersive in nature. Another severe limitation of this approach is that it is not possible to predict negative interactions. The geometric mean rule can be generalized by defining a term that measures the deviation from this assumption,[42] i.e., $C_{ij} = (1 - k_{ij})\delta_i\delta_j$. This leads to the following:

$$B_{ij} = (\delta_i - \delta_j)^2 + 2k_{ij}\delta_i\delta_j \tag{12}$$

where k_{ij} is a constant, small value compared to unity, characteristic of the unlike i/j pair interaction. As can be seen from eq 12, the effect of deviation from the geometric mean becomes less serious as the difference of the solubility parameters between the two components, $|\delta_i - \delta_j|$, becomes larger. However, it should be noted that even small deviations from the geometric mean assumption, especially when δ_i and δ_j are close to each other, can have an appreciable affect on the calculated B_{ij}. Equation 12 also makes it possible to estimate the binary interaction energies that are exothermic. According to Paul and Barlow,[35] only very slight departures from the geometric mean assumption are needed to achieve blend miscibility.

Experimental Section

Materials. The monomers MMA, S, and xA were washed with an aqueous sodium hydroxide solution, rinsed with distilled water, and then dried over calcium chloride. Polymers were synthesized by addition polymerization in bulk with AIBN as the initiator at 60 °C. The reaction times were adjusted to keep conversion less than 10% to avoid significant composition drift in the copolymer. All polymers were recovered by addition of an excess of methanol to the reaction mixture, purified by repeated chloroform/methanol reprecipitation, and dried in a vacuum oven for several days before characterization.

The methyl methacrylate and styrenic copolymers synthesized are listed in Table 1 and Table 2, respectively. The comonomer compositions of synthesized polymers were determined by ^{1}H NMR, and molecular weights were obtained by using gel permeation chromatography (GPC) calibrated with polystyrene standards. These copolymers were blended with various SAN copolymers, monodisperse PS homopolymers, and monodisperse PMMA homopolymers. The SAN copolymers of different AN compositions used in this study, and most of the PMMA and PS homopolymer standards are described elsewhere;[45,46] however, the poly(*n*-alkyl acrylates) and additional monodisperse PMMA and PS homopolymer standards used here are listed in Table 3. The density of the glassy polymers was determined at 30 °C by a density gradient column using $ZnCl_2$ solutions. The density of the rubbery polymers was obtained by a pycnometer according to the ASTM standard method; alcohol rather than water was used to eliminate errors due to air bubbles.

Blend Preparation. Blends containing equal masses of two-component copolymers (or polymers) were cast from dichloromethane solution at room temperature. These blends were then dried in a vacuum oven while increasing the temperature 20 °C every day until the designated annealing temperature 120 °C was reached, and thermodynamic equilibrium was further established.

Table 1. Methyl Methacrylate Copolymers Synthesized for This Study

abbreviation	wt % acrylate	$\bar{M}_n$	$\bar{M}_w$	T_g (°C)
PMMA	0	205 000	442 000	118
MMA-MA5	5.2	131 000	275 000	110
MMA-MA8	8.1	108 000	232 000	104
MMA-MA9	9.4	153 000	295 000	102
MMA-MA11	11.0	120 000	253 000	99
MMA-MA12	12.6	110 000	227 000	96
MMA-MA13	13.4	101 000	233 000	94
MMA-nPA7	7.0	163 000	302 000	100
MMA-nPA12	12.0	138 000	289 000	88
MMA-nPA18	18.0	123 000	247 000	76
MMA-nPA24	24.0	126 000	265 000	64
MMA-nPA31	31.0	156 000	323 000	50
MMA-nPA38	38.0	158 000	335 000	37
MMA-nHA9	9.2	230 000	550 000	89
MMA-nHA15	15.3	206 000	496 000	77
MMA-nHA21	21.1	241 000	525 000	63
MMA-nHA25	25.6	219 000	506 000	49
MMA-nHA31	31.0	187 000	406 000	38
MMA-nHA34	34.0	248 000	511 000	30
MMA-nHA45	45.6	271 000	596 000	11
MMA-nDA5	5.6	254 000	560 000	97
MMA-nDA10	10.6	223 000	503 000	77
MMA-nDA17	17.9	240 000	514 000	55
MMA-nDA21	21.2	242 000	524 000	46
MMA-nDA25	25.7	369 000	701 000	35
MMA-nDA28	28.9	226 000	463 000	27
MMA-nDA36	36.3	419 000	861 000	11

Table 2. Styrenic Copolymers Synthesized for This Study

abbreviation	wt % acrylate	$\bar{M}_n$	$\bar{M}_w$	T_g (°C)
S-MA11	11.0	162 000	341 000	92
S-MA17	17.8	142 000	357 000	86
S-MA26	26.0	206 000	419 000	80
S-MA30	30.4	185 000	378 000	75
S-MA37	37.0	156 000	369 000	69
S-EA18	18.1	152 000	323 000	73
S-EA27	27.4	146 000	338 000	55
S-EA32	32.1	154 000	330 000	52
S-EA36	36.8	155 000	373 000	46
S-EA43	43.2	192 000	430 000	38
S-nPA18	18.5	189 000	390 000	65
S-nPA26	26.1	192 000	396 000	52
S-nPA32	32.8	243 000	497 000	37
S-nPA36	36.3	209 000	425 000	31
S-nPA41	41.6	169 000	379 000	22
S-nBA27	27.9	185 000	361 000	43
S-nBA34	34.7	187 000	394 000	31
S-nBA40	40.2	189 000	378 000	22
S-nBA46	46.1	196 000	404 000	13
S-nBA53	53.3	224 000	452 000	2
S-nHA14	14.6	177 000	360 000	68
S-nHA18	18.1	182 000	381 000	58
S-nHA28	28.2	185 000	400 000	37
S-nHA33	33.9	171 000	357 000	26
S-nHA43	43.2	224 000	451 000	10
S-nDA12	12.9	146 000	303 000	68
S-nDA24	24.1	150 000	314 000	40
S-nDA31	31.6	173 000	350 000	25
S-nDA41	41.8	256 000	516 000	6
S-nDA48	48.9	264 000	534 000	−6

Blend Assessment. Glass transition temperatures (T_g) were determined to characterize the synthesized copolymers and assess blend miscibility using a Perkin-Elmer DSC-7 system at a scanning rate of 20 °C/min. Two scans were performed: the first scan was run up to the corresponding annealing temperature to erase thermal history, and a second run was made for thermal analysis. Visual determination of phase behavior was made before and after the annealing treatment for each blend. Whenever the glass transition temperatures of the two components of the blends were too close to each other, phase behavior was determined visually. Figure 1 shows the onset T_g for the synthesized copolymers with the solid lines representing the prediction of the Fox equation.

Table 3. Additional Polymer Standards Used in This Study[a]

polymer	$\bar{M}_w$	$\bar{M}_w/\bar{M}_n$	source
PS35000	35 000	<1.06	Pressure Chemical
PS52000	52 000	1.03	Polymer Laboratories
PMMA16700	16 700	1.06	Polymer Source, Inc.
PMMA27500	27 500	1.10	Polymer Source, Inc.
PMMA33500	33 500	1.07	Polymer Laboratories
PMMA60000	60 000	1.07	Polymer Laboratories
PMMA105400	105 400	1.04	Polymer Source, Inc.
PMMA1256000	1 256 000	1.16	Polymer Source, Inc.
PMA	49 800	3.69	Scientific Polymer
PnPA	139 800	3.05	Scientific Polymer
PnHA	85 700	3.43	Scientific Polymer
PnDA	123 400	3.64	Scientific Polymer

[a] Others have been described previously.[45,46]

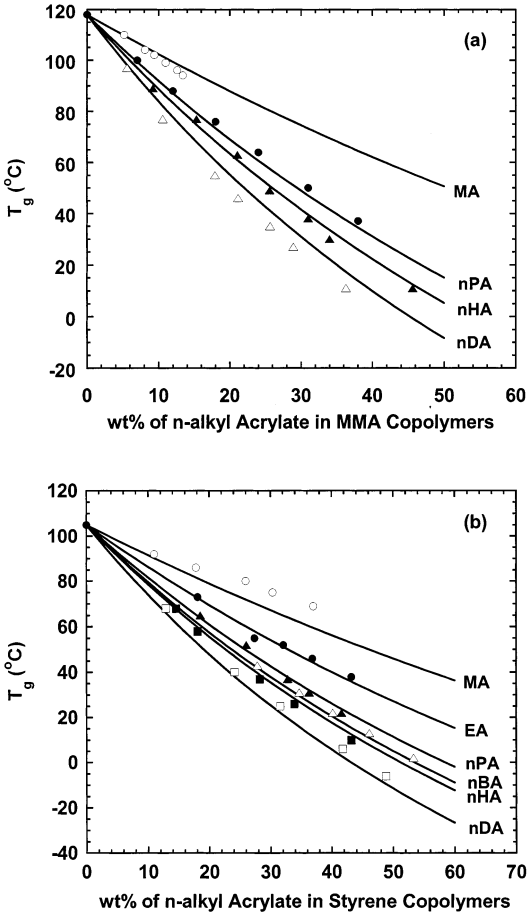

Figure 1. Glass transition temperatures (T_g) of synthesized copolymers vs copolymer compositions: (a) MMA/*n*-alkyl acrylate copolymers; (b) S/*n*-alkyl acrylate copolymers. Solid lines represent the prediction of the Fox equation.

PVT Measurement. A Gnomix PVT apparatus was used to obtain PVT data, from which the characteristic lattice fluid theory equation-of-state parameters were calculated according to the Sanchez−Lacombe equation-of-state expressed in terms of reduced properties:[23,47−49]

$$\tilde{\rho}^2 + \tilde{P} + \tilde{T}\left[\ln(1-\tilde{\rho}) + \left(1-\frac{1}{r}\right)\tilde{\rho}\right] = 0 \qquad (13)$$

where the chain length $r = MP^*/kT^*\rho^* = M/v^*\rho^*$, $\tilde{P} = P/P^*$, $\tilde{T} = T/T^*$, and $\tilde{\rho} = 1/\tilde{v} = \rho/\rho^*$. The variables with asterisks are characteristic parameters usually determined by fitting experimental PVT data for the homopolymers to eq 13 and applying mixing rules for copolymers. New experimental PVT data obtained in this study for PnPA, PnHA, and PnDA are reported elsewhere.[50] The Sanchez−Lacombe characteristic parameters determined from these data are listed in Table 4 along with those given in the literature for other relevant polymers in this study.[23]

Table 4. Sanchez−Lacombe Characteristic Parameters Used in This Study

polymer	T^* (K)	P^* (MPa)	ρ^* (g cm^{-3})	temperature range (°C)	reference
PS	751	397.0	1.1090	150−200	23
PS	810	373.0	1.0920	220−270	23
PMMA	728	503.0	1.2601	150−200	23
PMMA	742	509.0	1.2564	220−270	23
PAN	853	535.7	1.2299	150−200	23
PMA	665	542.0	1.2330	100	23
PEA	640	401.4	1.1857	37−217	23
PnPA	702	339.5	1.1630	120−210	this study
PnBA	646	378.8	1.1459	150−210	10
PnHA	659	339.0	1.0914	120−210	this study
PnDA	686	337.0	1.0340	120−210	this study

Results and Discussion

Critical Molecular Weight Experiments. As can be seen from eq 3, six different binary interaction energy densities, $B_{S/MMA}$, $B_{S/AN}$, $B_{MMA/AN}$, $B_{MMA/xA}$, $B_{S/xA}$, and $B_{AN/xA}$, are needed to completely describe the phase behavior for the blends of SAN copolymers with copolymers of MMA with an *n*-alkyl acrylate. However, three common binary interaction energy densities, i.e., $B_{S/AN}$, $B_{MMA/AN}$, and $B_{S/MMA}$, for all blends of this type have been reported previously in the literature.[10−12,17−20,51−54] Knowledge about the three remaining binary interaction energies for each of the current blend systems, viz. $B_{S/xA}$, $B_{MMA/xA}$, and $B_{xA/AN}$, is unknown.

In principle, estimates of $B_{S/xA}$ and $B_{MMA/xA}$ can be obtained by the critical molecular weight approach described in an earlier section.[10−12,24,30−33] In this technique, the molecular weights of the immiscible component polymers are reduced until the blend becomes miscible, resulting from the dominance of the favorable contribution of the entropy of mixing over the unfavorable enthalpy of mixing and other noncombinatorial effects. The critical interaction energy, $B_{critical}$, at the boundary between miscibility and immiscibility can be evaluated according to eq 2. Particularly, high molecular weight homopolymers of poly(methyl acrylate) (PMA), poly(*n*-propyl acrylate) (PnPA), poly(*n*-hexyl acrylate) (PnHA), and poly(*n*-decyl acrylate) (PnDA) were blended with monodisperse homopolymers of PS and PMMA standards of various molecular weights listed in Table 3 in this study. Only a brief description of the results is provided here since the details can be found elsewhere.[50]

Blends of PnHA with monodisperse PS having molecular weights above 1350 were found to be immiscible, while those with molecular weights below 800 were miscible; these observations led to $0.38 < B_{S/nHA} < 0.62$ cal/cm^3. Blends of PnHA with monodisperse PMMA with molecular weights above 14 000 were all determined to be immiscible, which suggests $B_{MMA/nHA} > 0.41$ cal/cm^3. Similarly, the procedure described above was used to obtain ranges for the interaction energy densities for other *n*-alkyl acrylates with MMA or S units; the results are summarized in Table 5. It should be noted that information about $B_{MMA/MA}$ obtained in this study agrees well with those reported in the literature.[55] The information contained in Table 5 is very useful once combined with the isothermal miscibility maps for evaluating values of all relevant binary interaction energy densities as will be illustrated in a later section. Nevertheless, this strategy could not be used to obtain information about $B_{xA/AN}$ due to the unavailability of

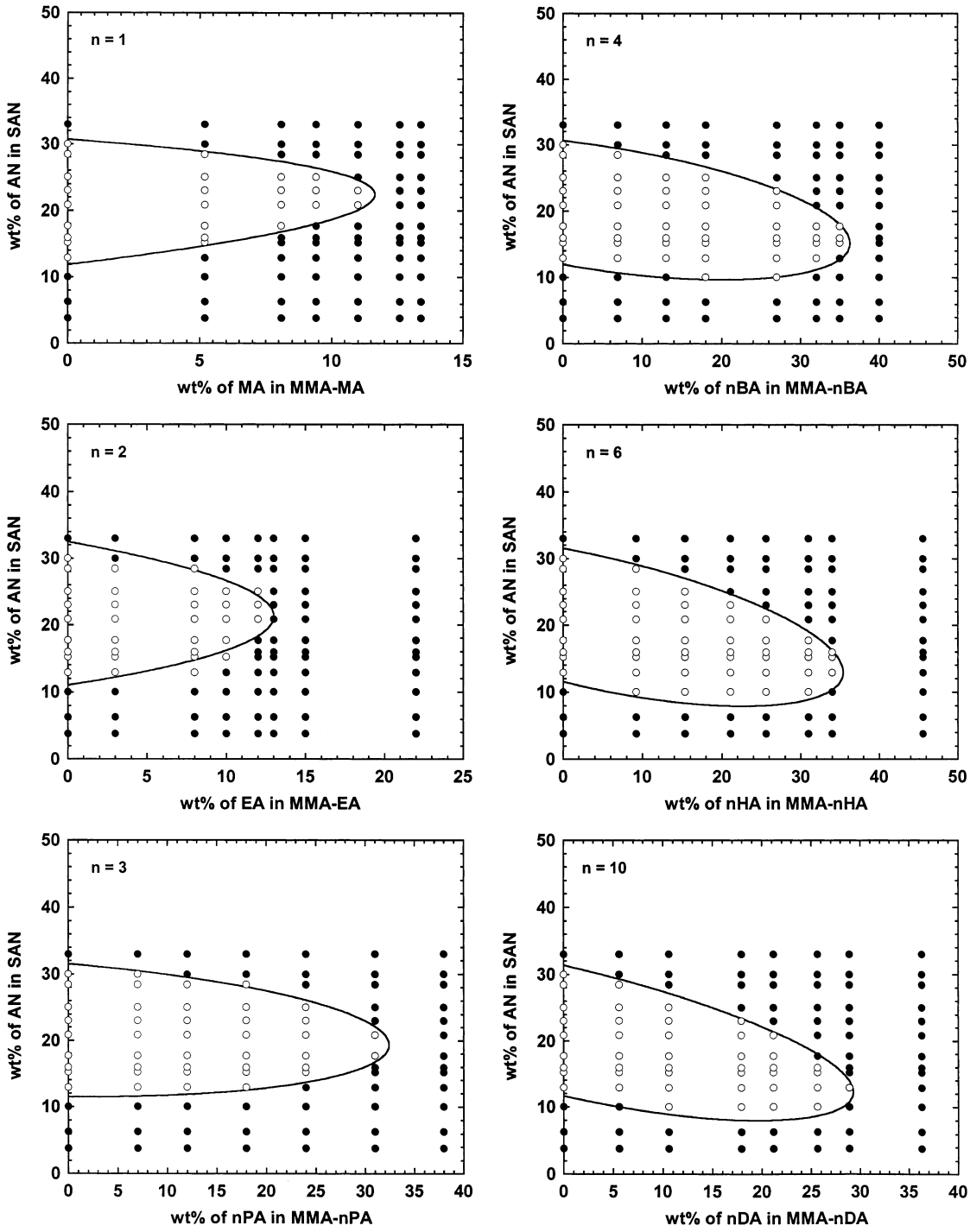

Figure 2. Copolymer miscibility maps at 120 °C for blends of MMA/*n*-alkyl acrylate copolymers with SAN copolymers: (○) miscible; (●) immiscible. The solid curve was calculated from the B_{ij} set obtained from the best fit of the miscibility map (see Table 6 for values).

Table 5. Results from Critical Molecular Weight Experiments

unit pairs	range of interaction energy densities
MMA/MA	$0.14 < B_{MMA/MA} < 0.26$
MMA/nPA	$0.24 < B_{MMA/nPA} < 0.39$
MMA/nHA	$B_{MMA/nHA} > 0.41$
MMA/nDA	$B_{MMA/nDA} > 0.39$
S/MA	$B_{S/MA} > 0.88$
S/nPA	$0.37 < B_{S/nPA} < 0.60$
S/nHA	$0.38 < B_{S/nHA} < 0.62$
S/nDA	$0.37 < B_{S/nDA} < 0.60$

monodisperse polyacrylonitrile (PAN) polymers as pointed out previously.[10]

Evaluation of Interaction Energy Densities by Copolymer Composition Mapping. For consistency with other recent work from this laboratory,[10] blends of MMA-*co*-MA/SAN, MMA-*co*-nPA/SAN, MMA-*co*-nHA/SAN, and MMA-*co*-nDA/SAN were prepared and evaluated at 120 °C. The isothermal miscibility phase maps at a temperature of 120 °C for blends of SAN copolymers and copolymers of methyl methacrylate (MMA) with methyl acrylate (MA), *n*-propyl acylate (nPA), *n*-hexyl acrylate (nHA), and *n*-decyl acrylate (nDA) are shown in Figure 2. For comparison purposes, the phase behavior of blends of SAN with copolymers of MMA with EA

Table 6. Interaction Energies (cal/cm^3) Determined by Copolymer Composition Mapping at 120 °C

interaction pair	blend systems: MMA-MA/SAN		MMA-EA/SAN		MMA-nPA/SAN		MMA-nBA/SAN		MMA-nHA/SAN		MMA-nDA/SAN		confidence limits for B_{ij} (cal/cm^3)
	ΔP^*_{ij}	B_{ij}	ΔP^*_{ij}	B_{ij}	ΔP^*_{ij}	B_{ij}	ΔP^*_{ij}	B_{ij}	ΔP^*_{ij}	B_{ij}	ΔP^*_{ij}	B_{ij}	
S/MMA	0.23	0.22	0.23	0.22	0.23	0.22	0.23	0.22	0.23	0.22	0.23	0.22	±0.02
MMA/AN	4.55	4.51	4.55	4.51	4.55	4.51	4.55	4.51	4.55	4.51	4.55	4.51	±0.25
S/AN	7.37	7.02	7.48	7.12	7.42	7.07	7.37	7.02	7.43	7.08	7.42	7.07	±0.36
MMA/MA	0.09	0.2											±0.03
S/MA	1.04	1.12											±0.06
MA/AN	3.71	4.2											±0.08
MMA/EA			−0.10	0.12									±0.06
S/EA			0.62	0.84									±0.06
EA/AN			4.52	5.09									±0.07
MMA/nPA					0.40	0.38							±0.05
S/nPA					0.49	0.49							±0.05
nPA/AN					5.71	5.66							±0.07
MMA/nBA							0.49	0.62					±0.09
S/nBA							0.17	0.39					±0.10
nBA/AN							6.49	6.81					±0.09
MMA/nHA									0.78	0.82			±0.06
S/nHA									0.28	0.42			±0.06
nHA/AN									7.60	7.68			±0.08
MMA/nDA											1.04	0.98	±0.10
S/nDA											0.45	0.49	±0.11
nDA/AN											8.67	8.47	±0.10

and nBA reported previously in this laboratory are reproduced in Figure 2 as well.[10] In all the phase maps, the open circles represent blends found to be miscible while the filled circles represent immiscible ones. As can be seen from Figure 2, pure PMMA was found to be miscible with SAN copolymers between 12.9 and 30 wt % AN, which agrees well with other literature.[1−12] All blends show a closed miscibility region, which means that there is a limit on the amount of any *n*-alkyl acrylate that can be incorporated into copolymers of MMA while maintaining miscibility with SAN; this limit varies with the *n*-alkyl chain length as suggested previously.[10] In other words, the size of the *n*-alkyl pendant group has a significant effect on the miscibility regions for blends of MMA-*co*-xA/SAN. This conclusion is made clear by the experimental observations that SAN copolymers are immiscible with MMA−MA copolymers containing 12.6 wt % or more of MA, 13 wt % or more of EA, 38 wt % or more of nPA, 40 wt % or more of nBA, 45.6 wt % or more of nHA, and 36.3 wt % or more of nDA. In contrast to MA and EA, addition of nPA, nHA, and nDA tends to skew the miscible region toward lower AN content of the SAN copolymer as found previously for EA and nBA;[10] furthermore, the miscible region is skewed toward lower AN content of the SAN copolymer as the *n*-alkyl chain length increases. From eq 3, this is due to the fact that the interaction energy between AN and xA, $B_{AN/xA}$, increases as the *n*-alkyl chain length increases, as will be discussed later.

Six interaction energy densities for each blend system can be obtained by fitting eqs 2 and 3 to the isothermal miscibility maps. In the fitting process, the $B_{critical}$ value is based on the assumption of constant molecular weights of the component copolymers along the miscible boundary. The corresponding $B_{critical}$ values for MMA-*co*-MA/SAN blends, MMA-*co*-nPA/SAN blends, MMA-*co*-nHA/SAN blends, and MMA-*co*-nDA/SAN blends are 0.0086, 0.0083, 0.0065, and 0.0064, respectively. However, the actual $B_{critical}$ values for each copolymer−copolymer pair can be calculated from the actual molecular weights and the results compared with the constant $B_{critical}$ as explained previously;[10] the detailed results can be found elsewhere.[50] Deviations from the fixed $B_{critical}$ value must be considered in the fitting of interaction parameters determined in this manner as noted previously.[10]

There are numerous methods that can be used to conduct the fitting process.[45,46,56] In this study, an improved computer program was written to obtain the interaction energy densities which best fit the experimental data using the Flory−Huggins criteria for miscibility. The value of $B_{S/MMA}$ was set equal to 0.22 cal/cm^3 at 120 °C as in previous studies.[10] This choice is consistent with extensive data available in the literature for the S/MMA pair.[10−12,17−19,51−54] The user needs to specify a range in which a given interaction energy may fall for the rest of the five pairs. This range can be easily determined by either critical molecular weight experiments as described earlier or roughly estimated by solubility parameters.[35] The user needs to specify the experimental data points along the miscibility boundary. Unlike the prior programs mentioned above, the computation does not include an arbitrary penalty for data points on the wrong side of the boundary, such as a miscible data point located in the immiscible region.[10] Instead, the maximum fraction of *n*-alkyl acrylate in the MMA-*n*-alkyl acrylate copolymers that produces miscibility with SAN copolymers was specified from the experimental data shown in Figure 2. For each set of interaction energies, within the specified ranges, the program constructs an objective function defined as the sum of the orthogonal distances between the data points along the miscibility border and the curve defined by eq 3 and then determines the set of B_{ij} that minimizes this function. The corresponding B_{ij} values obtained by fitting the thermodynamic theory independently of the experimental data for the blend systems are summarized in Table 6. The corresponding values of the Sanchez−Lacombe bare interaction energy ΔP^*_{ij}, computed from these values using eq 8, are also shown. The Sanchez−Lacombe equation-of-state characteristic parameters used in the calculation were taken from Table 4. All systems yield a value of 4.51 cal/cm^3 for the MMA/AN pair which agrees well with results from other studies.[37] For the S/AN interaction, the range of values from the different blend systems is found to

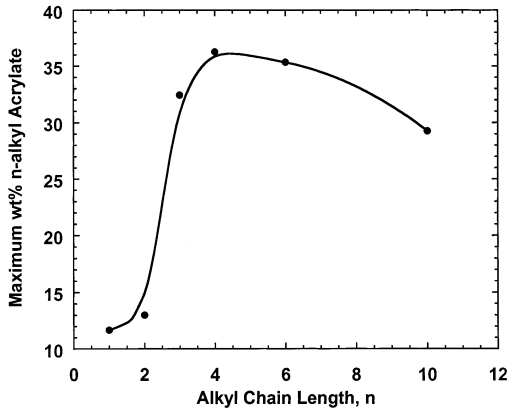

Figure 3. Plot of the maximum weight fraction of *n*-alkyl acrylate in copolymers with MMA that permits some level of miscibility with SAN copolymers vs the length of the *n*-alkyl chain.

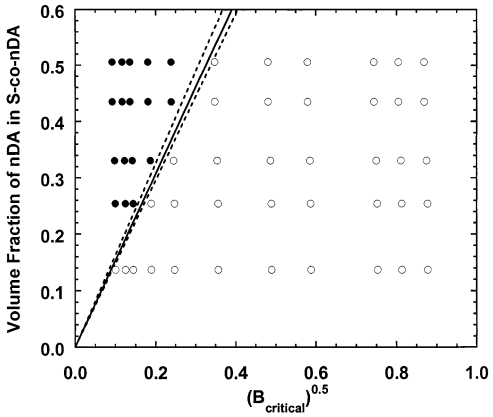

Figure 4. Isothermal miscibility maps at 120 °C for 50/50 blends of S/*n*-decyl acrylate copolymers with PS homopolymers of varying molecular weights plotted according to eq 6: (○) miscible; (●) immiscible. From the slope of the line separating the miscible and immiscible blends the following was calculated: $B_{S/nDA} = 0.43 \pm 0.05$ cal/cm^3 at 120 °C.

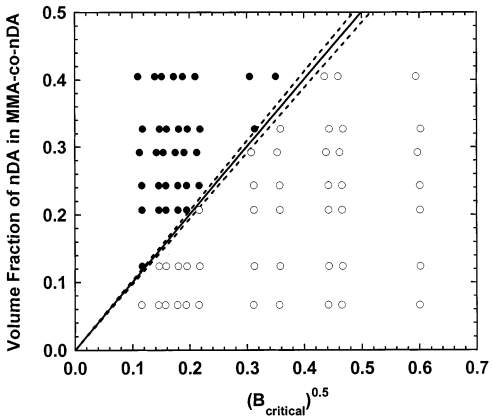

Figure 5. Isothermal miscibility maps at 120 °C for 50/50 blends of MMA/*n*-decyl acrylate copolymers with PMMA homopolymers of varying molecular weights plotted according to eq 7: (○) miscible; (●) immiscible. From the slope of the line separating the miscible and immiscible blends the following was calculated: $B_{MMA/nDA} = 1.00 \pm 0.06$ cal/cm^3 at 120 °C.

be 7.02−7.12 cal/cm^3; these values fall within the range reported previously.[20] The confidence limits for the calculated interaction energies, given in Table 6, were determined by adopting the same procedure reported previously,[10] i.e., by adjusting each interaction parameter and determining the limit to where an acceptable fit to the miscibility data could be found by changing the other parameters. The interaction energy density parameters for blends of MMA-*co*-EA/SAN and MMA-*co*-nBA/SAN reflect a refit of experimental data reported previously using the current methodology.[10]

The solid curves in Figure 2 were calculated using the best-fit parameters listed in Table 6. As can be seen, these curves agree well with the experimental data. The maximum amount of *n*-alkyl acrylate that can be tolerated in MMA copolymers while preserving some level of miscibility with SAN copolymers is plotted vs the number of carbon atoms in the *n*-alkyl pendant group in Figure 3. As pointed out earlier, this result is quite interesting since the limit does not show a simple monotonic decrease with the size of the alkyl group as might be expected but rather first increases, goes through a maximum, and then decreases. This trend is the result of the combined contributions of the six different interaction energy unit pairs, but especially from the S/xA, MMA/xA, and AN/xA pairs. An unanticipated trend in any one or a combination of the interaction energy density parameters with the *n*-alkyl chain length could significantly undermine the intuitive expectation that the limit simply decreases monotonically with the size of the alkyl group. Indeed, Table 6 shows that $B_{S/xA}$ and $B_{MMA/xA}$ both initially decrease and then increase with *n*-alkyl chain length, while $B_{AN/xA}$ increases monotonically with *n*-alkyl chain length. These trends in interaction energies along with *n*-alkyl chain length will be explored in more detail later.

Evaluation of Interaction Energy Densities by the Copolymer/Critical Molecular Weight Method. As discussed in previous sections, the copolymer composition mapping strategy has inherent drawbacks that the copolymer/critical molecular weight method avoids. Furthermore, the copolymer/critical molecular weight approach has the benefit of direct error limit analysis.[11,12,20] But the real advantage of this method is that it determines only one interaction parameter at a time and avoids compensation effects; thus, it is more accurate. The interactions between *n*-alkyl acrylate and S or MMA, i.e., $B_{S/xA}$ and $B_{MMA/xA}$, listed in Table 6 were all reexamined by this powerful strategy. A summary of these results is provided here; a more detailed discussion can be found elsewhere.[50]

Miscibility data for PS/S-nDA copolymer blends are plotted, in the manner suggested by eq 6, in Figure 4 for 120 °C where the open circles represent miscible blends and the closed circles represent immiscible blends. For the S-nDA copolymers containing 12.9 wt % nDA, all blends are miscible regardless of the molecular weight of the monodiperse PS. The blends containing PS with $\bar{M}_w = 35\,000$ g/mol are immiscible with S-nDA copolymers containing 24.1 wt % and more nDA. The blends of the PS with $\bar{M}_w = 9200$ g/mol did not become immiscible until the nDA content was 41.8 wt %.

The same type of plot for PMMA/MMA-nDA blends is constructed in Figure 5 for 120 °C. For the MMA-nDA copolymers containing the lowest nDA content (5.6 wt %), all blends are miscible regardless of the molecular weight of the monodiperse PMMA. The blends with the highest molecular weight PMMA (60 000 g/mol) were immiscible with MMA-nDA copolymers containing 10.6 wt % and more nDA. The blends of the PMMA with $\bar{M}_w = 5720$ g/mol did not become immiscible until the nDA content was 28.9 wt %.

Table 7. Interaction Energies (cal/cm^3) Determined by Copolymer/Critical Molecular Weight Method at 120°C

interaction pair	ΔP^*_{ij} (cal/cm^3)	B_{ij} (cal/cm^3)	error limits for B_{ij} (cal/cm^3)
MMA-MA	0.08	0.19	±0.02
MMA-EA	−0.07	0.15	±0.03
MMA-nPA	0.36	0.34	±0.04
MMA-BA	0.43	0.56	±0.06
MMA-nHA	0.74	0.78	±0.05
MMA-nDA	1.06	1.00	±0.06
S-MA	0.96	1.05	±0.07
S-EA	0.57	0.80	±0.06
S-nPA	0.44	0.44	±0.05
S-nBA	0.12	0.35	±0.04
S-nHA	0.23	0.38	±0.04
S-nDA	0.39	0.43	±0.05

In these plots of ϕ'_{nDA} (or ϕ''_{nDA}) vs $\sqrt{B_{critical}}$, straight lines passing through the origin can be drawn that well separate the miscible from the immiscible blends, see the solid lines in Figures 4 and 5. The error limits can be estimated by constructing the dashed lines shown. The values of $B_{S/nDA}$ and $B_{MMA/nDA}$ determined from the slopes of the various lines shown are 0.43 ± 0.05 and 1 ± 0.06 cal/cm^3, respectively. The corresponding values of $\Delta P^*_{S/nDA}$ and $\Delta P^*_{MMA/nDA}$ at 120 °C according to eq 8 are 0.39 ± 0.05 and 1.06 ± 0.06 cal/cm^3, respectively. The same procedure was applied to the other PS/S-*co*-*n*-alkyl acrylate and PMMA/MMA-*co*-*n*-alkyl acrylate blend systems. The complete interaction energy density parameters determined by this method are listed in Table 7. As can be seen from Tables 6 and 7, after refitting the binary interaction energy density parameters from the prior data,[10] there is only a slight difference between the interaction energy densities determined by the copolymer composition mapping approach and the copolymer/critical molecular weight method. This indicates that copolymer composition mapping strategy can achieve considerable accuracy provided that an appropriate fitting algorithm is employed while the copolymer/critical molecular weight approach is a generally more accurate and convenient alternative.

Trends in the Interaction Energies: $B_{MMA/xA}$, $B_{S/xA}$, and $B_{AN/xA}$. Chu et al. discussed the trends in the interaction energies of repeating unit pairs between various methacrylates or acrylates and S, MMA, or AN;[10] however, their conclusions were based on very little experimental data. This study was designed to make a more complete analysis of these trends in $B_{S/xA}$, $B_{MMA/xA}$, and $B_{AN/xA}$ as a function of the alkyl pendant group length and establish the reasons for these trends.

The interaction energy density for MMA with *n*-alkyl acrylate repeating units, $B_{MMA/xA}$, is plotted vs the *n*-alkyl chain length in Figure 6. Values from both experimental approaches mentioned earlier as well as those predicted by solubility parameter theory, see eq 11, are shown. Several group contribution methods can be used to calculate solubility parameters; however, the method selected does not dramatically alter the results. The method proposed by van Krevelen and Hoftyze was used here since it is the most comprehensive tabulation of molar cohesion parameters;[57] the calculated values for the relevant polymers in this study are shown in Figure 7.

The interaction energy densities for the S/*n*-alkyl acrylate repeating units, $B_{S/xA}$, and the AN/*n*-alkyl acrylate repeating units, $B_{AN/xA}$, are also plotted, in the same manner, against the *n*-alkyl chain length in Figure 8 and Figure 9, respectively. However, $B_{AN/xA}$ values by the copolymer/critical molecular weight method approach are not shown since they could not be determined.

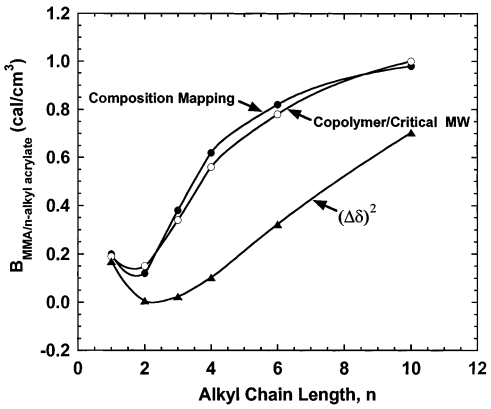

Figure 6. Effect of *n*-alkyl chain length on $B_{MMA/xA}$ values obtained from composition mapping and copolymer/critical molecular weight experiments (see Tables 6 and 7 for B_{ij} values). Values calculated from solubility parameters are also shown.

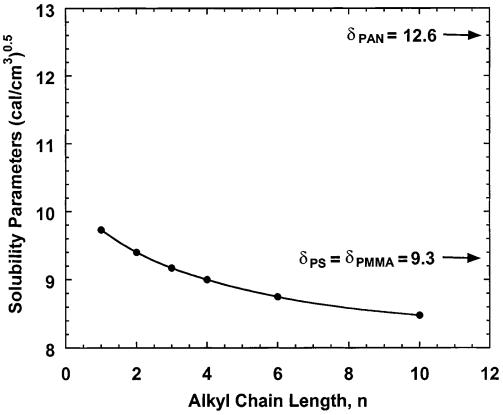

Figure 7. Solubility parameter (δ) for poly(*n*-alkyl acrylates) vs length of the *n*-alkyl chain. Solubility parameters for PAN, PS, and PMMA are shown for reference.

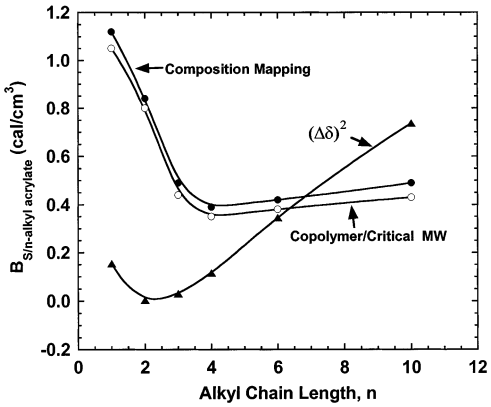

Figure 8. Effect of *n*-alkyl chain length on $B_{S/xA}$ values obtained from composition mapping and copolymer/critical molecular weight experiments (see Tables 6 and 7 for B_{ij} values). Values calculated from solubility parameters are also shown.

Figure 6 shows that $B_{MMA/xA}$, determined by both experimental methods, first decreases and then increases as the *n*-alkyl chain length increases; a minimum occurs at $n = 2$, i.e., for ethyl acrylate. The values from the two experimental techniques are generally in

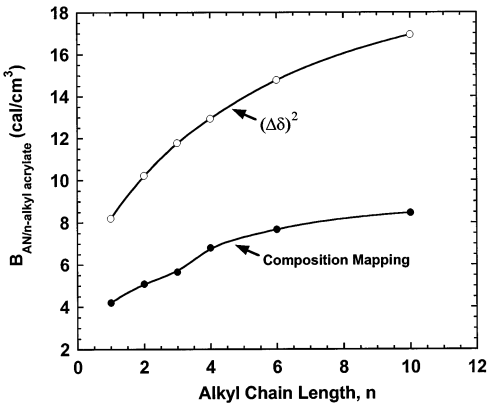

Figure 9. Effect of *n*-alkyl chain length on $B_{AN/xA}$ values obtained from composition mapping experiments (see Tables 6 and 7 for B_{ij} values). Values calculated from solubility parameters are also shown.

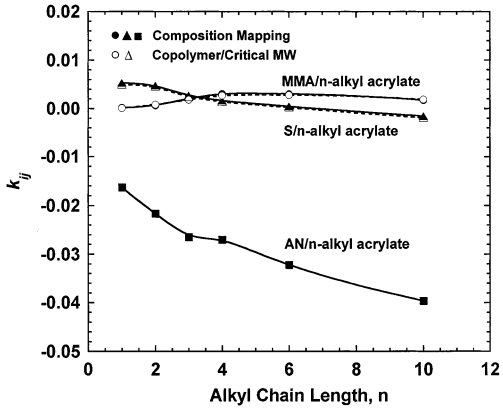

Figure 10. Effect of *n*-alkyl chain length on k_{ij} values calculated according to eq 12 (see Tables 6 and 7 for B_{ij} values).

excellent agreement. Values computed by the solubility parameter approach also show the same general trends; however, they are much lower than the experimental ones. Figure 8 shows a similar plot for the S/*n*-alkyl acrylates pairs. As *n* increases, $B_{S/xA}$ decreases rapidly and then increases slightly after reaching a minimum at $n = 4$. The solubility parameter method predicts that $B_{S/xA}$ has a minimum at $n = 2$; the predicted values are much lower than the experimental values at low *n* and then become larger than the experimental values at $n = 10$. It can be seen from Figure 8 that the values obtained by both experimental methods are in close agreement, and their differences are very consistent. The interaction energies between *n*-alkyl acrylates with acrylonitrile can be analyzed similarly; however, copolymer composition mapping is the only experimental strategy possible for this pair. The experimental results and those calculated from solubility parameters show that $B_{AN/xA}$ increases monotonically as the *n*-alkyl chain length increases. However, the value calculated from solubility parameters is much larger; this suggests that departures from the geometric mean assumption can have large effects on the estimates of B_{ij}. Again, this observation is quite consistent with the trends discussed previously.[10]

It should be emphasized that the qualitative trends in Figure 6, 8, and 9 are generally predicted by the solubility parameter method. From Figure 7, it is clear that the solubility parameter for AN is larger than that for *n*-alkyl acrylates for all values of *n*. Therefore, $B_{AN/xA}$ simply increases as *n* increases. On the other hand, the solubility parameter for the *n*-alkyl acrylate repeat unit is larger than that for S and MMA repeat units when *n* is small but falls below their level as *n* increases. Consequently, $B_{S/xA}$ and $B_{MMA/xA}$ decrease first and then increase as *n*-alkyl chain length increases. These facts also further support the earlier explanation of the trend in Figure 3.

While the binary interaction energy densities calculated from solubility parameters show the correct general trend with the size of the pendant *n*-alkyl group, the quantitative agreement with experimental values is quite poor. As pointed out earlier, this quantitative failure of the solubility parameter theory no doubt reflects departure from the simple geometric mean rule. This failure should not be surprising for the current systems since fundamentally this simplification only applies for nonpolar systems. The deviations from the geometric mean assumption are examined in this context below.

Values of k_{ij} were calculated from eq 12 for the *i*, *j* pairs of interest here. The k_{ij} related to the three common interaction pairs are found to be $k_{MMA/AN} = -0.0265$, $k_{S/MMA} = 0.001\,26$, and $k_{S/AN} = -0.0152$; those involving the various *n*-alkyl acrylate units are plotted vs the *n*-alkyl chain length in Figure 10. Values of B_{ij} determined by both the copolymer composition mapping and copolymer/critical molecular weight methods were used in these calculations. As can be seen, $k_{MMA/xA}$ is always a small positive value, and as the *n*-alkyl chain length *n* increases, it gradually increases up to $n = 4$ and then remains essentially a constant for nBA, nHA, and nDA. On the other hand, $k_{S/xA}$ begins as a small positive value and gradually decreases with *n* to become slightly negative for nDA. All $k_{AN/xA}$ have relatively large negative values that become even more negative as the *n*-alkyl chain length increases. The absolute value of $k_{AN/xA}$ is much larger than that of $k_{MMA/xA}$ and $k_{S/xA}$.

As pointed out earlier, the contributions of the heat of mixing and other noncombinatorial entropic effects are lumped into B. Thus, the k_{ij} calculated from eq 12 includes both enthalpic and entropic terms. The enthalpic contribution to k_{ij} for several interaction pairs were computed from the heat of mixing data previously determined in this laboratory via analogue calorimetry experiments.[58−61] These calculations show that the enthalpic term dominates. Therefore, in the following discussion, the entropic contribution will be neglected as we examine the deviation of the geometric mean assumption in terms of differences in molecular characteristics between repeat units.

An appropriate explanation of the above trends between k_{ij} and *n*-alkyl chain length requires careful examination of the geometric mean assumption introduced by London.[44] In this simplified treatment, the dispersion forces between molecules *i* and *j* at large separation are given by[44]

$$\Gamma_{ij} = (\Gamma_{ii}\Gamma_{jj})^{1/2} \tag{14}$$

where the Γ are the potential energies for the molecular pairs. The geometric mean rule assumes the molecular separation is large compared to the molecular diameters in addition to neglecting of polar and specific interactions.[44,62] Furthermore, Γ is a molecular quantity while the cohesive energy density *C* is an ensemble quantity; it is, therefore, not surprising that the geometric mean expression often fails and that the direction and extent

Table 8. Characteristics of Monomeric Units of Interest in This Study

monomer	μ (D)[68]	v (Å^3)[a]	α (10^{-24} cm^3)[68]	first I (eV)[68]
S	0.12	164.42	15.00	8.46
MMA	1.67	141.88		9.70
AN	3.92	74.31	8.05	10.91
MA	1.77	117.02	8.97	9.90
EA		148.21		
nPA		172.04		
nBA		196.74		
nHA		251.42		
nDA		359.10		

[a] Molecular volume calculated as v (Å^3) = 1.66 × [monomeric unit molar mass (g/mol)]/polymer density (g/cm^3).

of the deviations are unpredictable.[62] The most that can be done is to establish empirical trends. As pointed out by Barton,[62,63] Prausnitz et al.,[42] and other authors,[64−67] k_{ij} tends to be zero or positive for weakly polar systems but negative when the components form complexes or have very different shapes. They suggest that the absolute value of k_{ij} becomes larger as the differences in molecular size and chemical nature of the components increase. In other words, departure from the geometric mean assumption stems from a combination of factors, especially the chemical nature (e.g., molecular polarity and molecular size) of the relevant components. It should be noted, of course, that these molecular characteristics can be related to each other. In the following, the molecular factors that contribute to the departure from the geometric mean rule will be identified, and then the trends in Figure 10 will be interpreted in terms of the corresponding molecular characteristics of the components.

To see which factors contribute to k_{ij} requires revisiting of the well-known equations that describe the interaction energies between molecular species. The average potential energies $\bar{\Gamma}_{ij}$ between two molecules i and j in a vacuum due to dipole−dipole, dipole−induced dipole, and dispersion forces can be expressed by eqs 15, 16, and 17,[42] respectively

$$\bar{\Gamma}_{ij} = -\frac{2}{3}\frac{\mu_i^2\mu_j^2}{(4\pi\epsilon_0)^2 kTr^6} + ... \tag{15}$$

$$\bar{\Gamma}_{ij} = -\frac{\alpha_i\mu_j^2 + \alpha_j\mu_i^2}{(4\pi\epsilon_0)^2 r^6} \tag{16}$$

$$\bar{\Gamma}_{ij} = -\frac{3}{2}\frac{\alpha_i\alpha_j}{(4\pi\epsilon_0)^2 r^6}\left(\frac{I_iI_j}{I_i + I_j}\right) \tag{17}$$

where μ is the dipole moment, α is the polarizability, I is the first ionization potential, T is the absolute temperature, r is the distance between two molecules, and ϵ_0 is the dielectric permittivity of a vacuum. Dipole−dipole forces are essentially electrostatic in nature and exist only if both molecules have permanent dipoles while the dispersion forces are present in all polar and nonpolar molecules. As demonstrated by London[44] and Prausnitz et al.,[42] the contribution of induction forces to the overall intermolecular forces is relatively quite small regardless of the polarity of the molecules and will be neglected in the following discussion. On the other hand, dispersion forces overwhelmingly dominate in both nonpolar−nonpolar and nonpolar−weakly polar systems, while both dipole−dipole and dispersion forces are significant for polar−polar systems.

Therefore, polarity, polarizability, and first ionization potential are the three major factors that contribute to k_{ij}. For typical molecules, α is roughly proportional to molecular size while I does not vary to any great extent. The dipole moment μ, polarizability α, first ionization energy I, and molecular volume v for the various monomer units of interest here are listed in Table 8. For the S/xA pairs, the contribution of dipole−dipole forces to $k_{S,xA}$ is negligible since S is nearly nonpolar and n-alkyl acrylates are only weakly polar. When dispersion forces dominate, an expression for k_{ij} can be derived from eq 17 in terms of the first ionization potentials of molecules i and j

$$k_{ij} = 1 - \frac{2}{\beta + \frac{1}{\beta}} \tag{18}$$

where $\beta = \sqrt{I_i/I_j}$. Equation 18 can be used to qualitatively explain the trend of $k_{S/xA}$ with the n-alkyl chain length. The first ionization potential, I_{xA}, for n-alkyl acrylate is greater than that for styrene I_S, and it slightly decreases as the n-alkyl chain length increases.[68] This is due to the fact that the removal of the first electron from an uncharged n-alkyl acrylate molecule is easier, and the subsequent cation is more stable the longer the side chain. These facts can be further supported by the observation that the first ionization potential I for a certain homologous compound generally decreases as the chain grows.[68] Calculations from eq 18 suggest that $k_{S/xA}$ decreases slightly when the n-alkyl pedant group becomes larger. This is consistent with the experimental observation in Figure 10.

For AN/xA and MMA/xA pairs, as pointed out earlier, both dipole−dipole and dispersion forces are of importance. For the contribution from dispersion forces, a similar analysis can be performed. All I_{xA} are less than I_{AN} and almost equal to I_{MMA}. Calculations using eq 18 show that $k_{MMA/xA}$ is very small and almost a constant, while the absolute values of $k_{AN/xA}$ slightly increase as the side chains become larger. However, the magnitudes of the contribution from dispersion forces for the AN/xA pairs are much larger than that for the MMA/xA pairs. This is not surprising since the first ionization potential for AN is somewhat larger than that for MMA and n-alkyl acrylates. This observation can be further supported by the experimental evidence in Figure 10. The contributions from dipole−dipole forces for the AN/xA and MMA/xA pairs can be understood in terms of the difference in polarity between components i and j. Generally, the absolute value of k_{ij} increases as the polarity difference increases as demonstrated by Helpinstill and Van Winkle.[69] Because of insufficient data on dipole moments, solubility parameters are employed in the following discussion since polarity contributes to a larger cohesive energy density. To explore the possibility that differences in monomer unit polarity are linked to the departure from the geometric mean assumption, k_{ij} is replotted vs the absolute value of the difference in solubility parameters of components i and j, $|\Delta\delta_{ij}|$, for AN/xA and MMA/xA pairs in Figure 11. Except for the MMA/MA and MMA/nDA pairs, the absolute value of k_{ij} generally increases as $|\Delta\delta_{ij}|$ increases. This trend is especially evident when the polarity difference between monomer segments is larger as seen for AN/xA pairs.

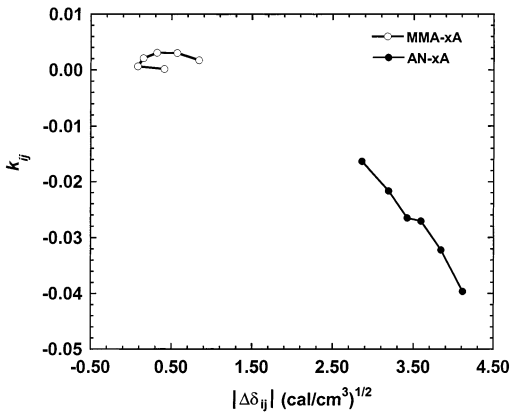

Figure 11. Effect of differences in repeat unit solubility parameters, $|\Delta\delta_{ij}|$, on k_{ij} values for AN/xA and MMA/xA pairs (see Figure 10 for k_{ij} values).

In other words, the magnitude of the contribution from dipole−dipole forces becomes more significant as $|\Delta\delta_{ij}|$ becomes bigger. The trends in Figure 11 are consistent with the proposed effect of polarity difference on k_{ij}; however, other interpretations are no doubt possible.

For the current systems, it appears that differences in the first ionization potential and in the polarity of the repeat units *i* and *j* are major contributors to the departure from the geometric mean assumption. In general, mismatch of monomer molecular characteristics is the key as concluded by Prausnitz et al.[42]

Conclusions

The miscibility regions for blends of styrene−acrylonitrile (SAN) copolymers and methyl methacrylate (MMA) copolymers with methyl acrylate (MA), *n*-propyl acrylate (nPA), *n*-hexyl acrylate (nHA), and *n*-decyl acrylate (nDA) were determined at 120 °C. The observed miscibility window depends strongly upon the nature of the *n*-alkyl pendant group and in ways that are not intuitively obvious. For example, the maximum composition of *n*-alkyl acrylate in MMA−*n*-alkyl acrylate copolymers that SAN can tolerate for miscibility initially increases and then decreases as the *n*-alkyl chain length increases (see Figure 3). The copolymer composition mapping approach was used to evaluate the relevant binary interaction energy densities using the Flory−Huggins theory combined with the binary interaction model. A more accurate alternative, the copolymer/critical molecular weight method, was also employed to determine the MMA/*n*-alkyl acrylate (xA) and the S/xA interaction energy densities. Of course, the latter requires the availability of a series of monodisperse homopolymers of widely varying molecular weight. The values of the interaction energies determined by the two methods agreed very well with each other when an appropriate data fitting algorithm was employed.

Tables 6 and 7 list the interaction energy densities determined in this study. The values for the MMA/xA and S/xA pairs were observed to initially decrease and then increase as the *n*-alkyl acrylate chain length increases; the AN/xA interaction energy density was found to increase monotonically with the size of the pendant *n*-alkyl group. These trends are qualitatively predicted by the simple solubility parameter theory; however, the absolute predictions are quite different than the experimentally determined parameters.

Figure 10 shows the trends of the deviations from the geometric mean assumption involving the various *n*-alkyl acrylate units, $k_{S/xA}$, $k_{MMA/xA}$, and $k_{AN/xA}$, vs the *n*-alkyl chain length. The $k_{MMA/xA}$ was observed to gradually increase up to $n = 4$ as the *n*-alkyl chain length *n* increases and then remains essentially a constant for nBA, nHA, and nDA; the $k_{S/xA}$ was found to decrease with *n*; all $k_{AN/xA}$ were seen to have relatively large negative values and became even more negative as the *n*-alkyl side chain grows. The trends in k_{ij} were discussed in terms of differences in monomer molecular characteristics, especially polarity, monomer size, and the first ionization potential. Molecular characteristic mismatch appears to be a significant contributing factor.

Acknowledgment. This research was funded by National Science Foundation Grant DMR 97-26484 administered by the Division of Materials Research-Polymers Program.

References and Notes

(1) Nishimoto, M.; Keskkula, H.; Paul, D. R. *Polymer* **1989**, *30*, 1279.
(2) Nishimoto, M.; Keskkula, H.; Paul, D. R. *Macromolecules* **1990**, *23*, 3633.
(3) Suess, M.; Kressler, J.; Kammer, H. W. *Polymer* **1987**, *28*, 957.
(4) Kressler, J.; Kammer, H. W.; Klostermann, K. *Polym. Bull. (Berlin)* **1986**, *15*, 113.
(5) Stein, D. J.; Jung, R. H.; Illers, K. H.; Hendus, H. *Angew. Makromol. Chem.* **1974**, *36*, 89.
(6) Fowler, M. E.; Barlow, J. W.; Paul, D. R. *Polymer* **1987**, *28*, 1177.
(7) Chiou, J. S.; Paul, D. R.; Barlow, J. W. *Polymer* **1982**, *23*, 1543.
(8) Cowie, J. M. G.; Lath, D. *Makromol. Chem., Macromol. Symp.* **1988**, *16*, 103.
(9) Callaghan, T. A. Ph.D. Dissertation, The University of Texas at Austin, 1992.
(10) Chu, J. H.; Paul, D. R. *Polymer* **1999**, *40*, 2687.
(11) Chu, J. H.; Paul, D. R. *Polymer* **2000**, *41*, 7193.
(12) Chu, J. H.; Tilakaratne, H. K.; Paul, D. R. *Polymer* **2000**, *41*, 5393.
(13) Merfeld, G. D.; Maa, T. T.; Chan, K.; Paul, D. R. *Polymer* **1999**, *41*, 663.
(14) Merfeld, G. D.; Chan, K.; Paul, D. R. *Macromolecules* **1999**, *32*, 429.
(15) Gan, P. P.; Paul, D. R. *J. Appl. Polym. Sci.* **1994**, *54*, 317.
(16) Nishimoto, M.; Keskkula, H.; Paul, D. R. *Polymer* **1991**, *32*, 1274.
(17) Gan, P. P.; Paul, D. R. *Polymer* **1994**, *35*, 3513.
(18) Gan, P. P.; Paul, D. R.; Padwa, A. R. *Polymer* **1994**, *35*, 3351.
(19) Gan, P. P.; Paul, D. R.; Padwa, A. R. *Polymer* **1994**, *35*, 1487.
(20) Zhu, S.; Paul, D. R. *Macromolecules* **2002**, *35*, 2078.
(21) Flory, P. J. *J. Chem. Phys.* **1942**, *10*, 51.
(22) Huggins, M. L. *J. Chem. Phys.* **1941**, *9*, 440.
(23) Stone, M. T.; Sanchez, I. C. Statistical Thermodynamics of Polymer Solutions and Blends. In *Polymer Blends: Formulation and Performance*; Bucknall, C. B., Ed.; John Wiley & Sons: New York, 2000; Vols. 1 and 2.
(24) Callaghan, T. A.; Paul, D. R. *Macromolecules* **1993**, *26*, 2439.
(25) Koningsveld, R.; Chermin, H. A. G.; Gordon, M. *Proc. R. Soc. London, Ser. A* **1970**, *319*, 331.
(26) Koningsveld, R.; Kleintjens, L. A.; Schoffeleers, H. M. *Pure Appl. Chem.* **1974**, *39*, 1.
(27) Koningsveld, R. *Br. Polym. J.* **1975**, *7*, 435.
(28) Koningsveld, R.; Kleintjens, L. A. *J. Polym. Sci., Polym. Symp.* **1977**, *61*, 221.
(29) Salomons, W.; Ten Brinke, G.; Karasz, F. E. *Polym. Commun.* **1991**, *32*, 185.
(30) Kambour, R. P.; Bendler, J. T.; Bopp, R. C. *Macromolecules* **1983**, *16*, 753.
(31) Kambour, R. P.; Gundlach, P. E.; Wang, I. C. W.; White, D. M.; Yeager, G. W. *Polym. Commun.* **1988**, *29*, 170.
(32) Callaghan, T. A.; Takakuwa, K.; Paul, D. R.; Padwa, A. R. *Polymer* **1993**, *34*, 3796.
(33) Takakuwa, K.; Gupta, S.; Paul, D. R. *J. Polym. Sci., Part B: Polym. Phys.* **1994**, *32*, 1719.
(34) Merfeld, G. D.; Paul, D. R. *Polymer* **1999**, *41*, 649.
(35) Paul, D. R.; Barlow, J. W. *Polymer* **1984**, *25*, 487.

(36) ten Brinke, G.; Oudhuis, L.; Ellis, T. S. *Thermochim. Acta* **1994**, *238*, 75.
(37) Merfeld, G. D. Polymer−Polymer Interactions Based on Mean Fileld Approximations. In *Polymer Blends: Formulation and Performance*; Bucknall, C. B., Ed.; John Wiley & Sons: New York, 2000; Vols. 1 and 2, Chapter 3.
(38) Kim, C. K.; Paul, D. R. *Polymer* **1992**, *33*, 1630.
(39) Jeon, K. S.; Char, K.; Kim, E. *Polym. J.* **2000**, *32*, 1.
(40) Scatchard, G. *Chem. Rev.* **1931**, *8*, 321.
(41) Hildebrand, J. H.; Prausnitz, J. M.; Scott, R. L. *Regular and Related Solutions. The Solubility of Gases, Liquids, and Solids*; Van Nostrand Reinhold: New York, 1970.
(42) Prausnitz, J. M.; Lichtenthaler, R. N.; Gomez de Azevedo, E. *Molecular Thermodynamics of Fluid-Phase Equilibria*, 3rd ed.; Prentice-Hall: Upper Saddle River, NJ, 1999.
(43) Berthelot, D. *Compt. Rend.* **1898**, *126*, 1703, 1857.
(44) London, F. *Trans. Faraday Soc.* **1937**, *33*, 8.
(45) Chu, J. H. Ph.D. Dissertation, The University of Texas at Austin, 1999.
(46) Merfeld, G. D. Ph.D. Dissertation, The University of Texas at Austin, 1998.
(47) Sanchez, I. C.; Lacombe, R. H. *J. Phys. Chem.* **1976**, *80*, 2352.
(48) Sanchez, I. C.; Lacombe, R. H. *J. Polym. Sci., Polym. Lett. Ed.* **1977**, *15*, 71.
(49) Sanchez, I. C.; Lacombe, R. H. *Macromolecules* **1978**, *11*, 1145.
(50) Zhu, S. Ph.D. Dissertation, The University of Texas at Austin, 2003.
(51) Fukuda, T.; Nagata, M.; Inagaki, H. *Macromolecules* **1984**, *17*, 548.
(52) Fukuda, T.; Nagata, M.; Inagaki, H. *Macromolecules* **1986**, *19*, 1411.
(53) Russell, T. P. *Macromolecules* **1993**, *26*, 5819.
(54) Brannock, G. R.; Barlow, J. W.; Paul, D. R. *J. Polym. Sci., Part B: Polym. Phys.* **1991**, *29*, 413.
(55) Cowie, J. M. G.; Ferguson, R.; Fernandez, M. D.; Fernandez, M. J.; McEwen, I. J. *Macromolecules* **1992**, *25*, 3170.
(56) Gan, P. P.; Paul, D. R. *J. Appl. Polym. Sci.* **1994**, *54*, 317.
(57) Van Krevelen, D. W. *Properties of Polymers. Their Estimation and Correlation with Chemical Structure*, 2nd ed.; Elsevier Scientific Publishing: New York, 1976.
(58) Ziaee, S.; Paul, D. R. *J. Polym. Sci., Part B: Polym. Phys.* **1996**, *34*, 2641.
(59) Ziaee, S.; Paul, D. R. *J. Polym. Sci., Part B: Polym. Phys.* **1997**, *35*, 831.
(60) Ziaee, S.; Paul, D. R. *J. Polym. Sci., Part B: Polym. Phys.* **1997**, *35*, 489.
(61) Fernandes, A. C. Ph.D. Dissertation, The University of Texas at Austin, 1986.
(62) Barton, A. F. M. *Chem. Rev.* **1975**, *75*, 731.
(63) Barton, A. F. M. *CRC Handbook of Solubility Parameters and Other Cohesion Parameters*; CRC Press: Boca Raton, FL, 1983.
(64) Funk, E. W.; Prausnitz, J. M. *Ind. Eng. Chem.* **1970**, *62*, 8.
(65) Null, H. R.; Palmer, D. A. *Chem. Eng. Prog.* **1969**, *65*, 47.
(66) Preston, G. T.; Prausnitz, J. M. *Ind. Eng. Chem. Process Des. Dev.* **1970**, *9*, 264.
(67) Weimer, R. F.; Prausnitz, J. M. *Hydrocarbon Process. Pet. Refin.* **1965**, *44*, 237.
(68) *Handbook of Chemistry and Physics*, 3rd electronic ed.; CRC Press: Boca Raton, FL, 2000.
(69) Helpinstill, J. G.; Van Winkle, M. *Ind. Eng. Chem. Process Des. Dev.* **1968**, *7*, 213.

MA020770Q